ChemComm

Accepted Manuscript

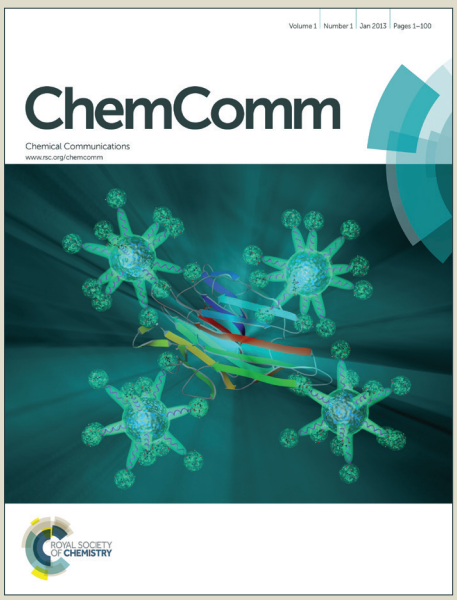

ROYAL SOCIETY OF CHEMISTRY

www.rsc.org/chemcomm

ChemComm

RSCPublishing

COMMUNICATION

An *In situ* Vapour Phase Hydrothermal Surface Doping Approach for Fabrication of High Performance Co_3O_4 Electrocatalyst with Exceptionally High S-doped Active Surface

Cite this: DOI: 10.1039/xoxxoooooox

Received ooth January 2012,
Accepted ooth January 2012

DOI: 10.1039/xoxxoooooox

www.rsc.org

Zhijin Tan,[a] Porun Liu,[*a] Haimin Zhang,[a, b] Yun Wang,[a] Mohammad Al-Mamun,[a] Hua Gui Yang,[a] Dan Wang,[a] Zhiyong Tang[a] and Huijun Zhao[*a, b]

A facile *in situ* vapour phase hydrothermal (VPH) surface doping approach has been developed for fabrication of high performance S-doped Co_3O_4 electrocatalyst with an unprecedentedly high surface S content (>47%). The demonstrated VPH doping approach could be useful for enrichment of surface active sites for other metal oxide electrocatalysts.

Electrocatalyst plays a critical role in energy conversion technologies such as solar and fuel cells. To date, high performance electrocatalysts used for these applications are mainly fabricated by noble metals that are precious and scarce, hindering their widespread use. Extensive efforts have therefore been made to develop non-precious-metal-based electrocatalysts using transition metal alloys, oxides, chalcogenides, nitrides, phosphides, carbides and metal/organic composites.[1]

For developing non-precious-metal-based high performance electrocatalysts, a central task is the pursuit of effective and efficient means to introduce rich catalytic active sites into the materials. Various active site creation/enrichment strategies have been reported such as morphological control, surface engineering and anchoring onto porous supports.[2] Among them, introducing exterior elements into existing material structures (doping) has been proven to be an effective approach.[3] Furthermore, available evidences suggest that the richness of active sites in the resultant electrocatalyst closely depends on the dopant content.[4] However, introducing a high dopant content via the majority of the reported bulk doping approaches is highly challenging because high dopant contents are destructive to the original crystal structures.[5] This is particularly true for anions doped electrocatalysts where the maximum dopant contents are generally less than 10%.[3a, 6]

It is well known that the activity of an electrocatalyst is determined by its surface active sites rather than those bulk ones.[7] Therefore, developing new doping approaches to realise selective surface high-content doping and non-destructive to the bulk material structures is highly desirable.

In this work, we venture to extend the VPH methods[8] for selective doping high content of exterior anion elements on the surface of metal oxides. Sulphur and spinel-type cobalt oxide (Co_3O_4) are respectively used as the anion dopant and bulk metal oxide to demonstrate the effectiveness of the proposed doping approach. An unprecedented 47% doped S content on the surface of Co_3O_4 nanosheets can be achieved, leading to a dramatically enhanced electrocatalytic performance. Although versatile applications of Co_3O_4 in catalysis have been reported,[9] the anion-doped Co_3O_4 catalysts have rarely been investigated.[6b, 10]

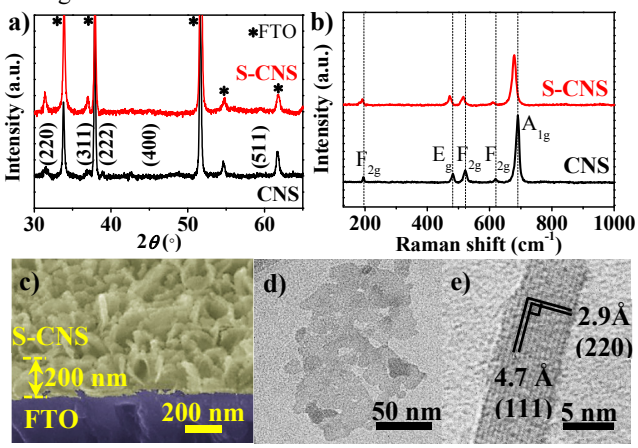

Fig. 1 (a) XRD patterns, (b) Raman spectra of CNS and S-CNS samples; (c) Cross-sectional SEM, (d) TEM and (f) HRTEM image of S-CNS sample.

The Co_3O_4 nanosheets coated FTO (denoted as "CNS") was firstly prepared via electrodeposition followed by sintering. Fig. S1 schematically illustrates the *in situ* VPH doping approach. Briefly, the synthesised CNS as the doping substrate is suspended in a VPH reactor containing Al_2S_3 and a small quantity of water as the doping reactants. The VPH doping is

carried out at a low temperature of 90°C for 6 h to obtain the S-doped Co_3O_4 nanosheets (denoted as "S-CNS"). An initial heating will generate water vapour, triggering a slow hydrolysis reaction of Al_2S_3 to produce H_2S gas that acts as the S doping source.

X-ray diffraction (XRD) data of the samples before and after VPH doping treatment show similar diffraction patterns (Fig. 1a) that can be assigned to spinel Co_3O_4 crystal structure (cubic, a = 8.056 Å, space group *Fd-3m*, JCPDS: PDF-74-1656, ICSD: 27497). However, the S-CNS sample shows diffraction peaks being slightly shifted ($\Delta 2\theta = 0.15°$) towards lower angle due to the increased lattice constants resulting from S doping.[11] These results confirm that there is no significant change in the bulk crystal structures of S-CNS sample. The room-temperature Raman spectra of both samples reveal 5 distinctive peaks ascribable to spinel Co_3O_4 crystals (Fig. 1b).[12] Notably, compared to CNS, all peaks observed from S-CNS appear at lower frequencies, indicating an increases surface structural disorder and decreased bond strength of S-doped Co_3O_4.

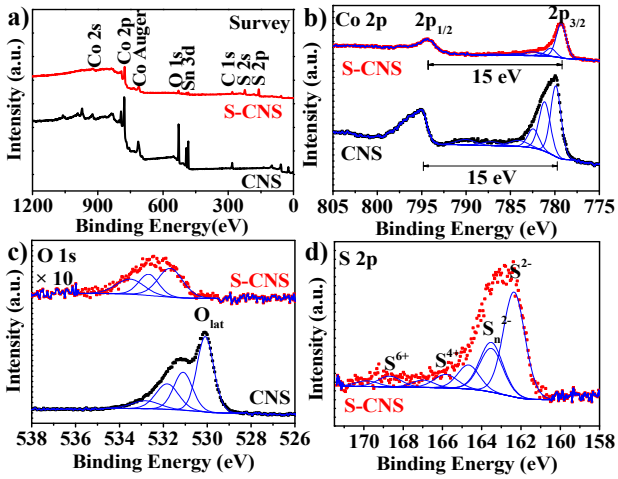

Fig. 2 XPS data: (a) survey spectra, (b) Co 2p and (c) O 1s spectra of CNS and S-CNS samples; (d) S 2p spectrum of S-CNS sample.

Scanning electron microscopic (SEM) observations of the samples before (Fig. S2) and after (Fig. 1c) S doping confirm that CNS and S-CNS samples are composed of a 200 nm layer of uniformly coated nanosheets (~6 nm in thickness) and the VPH doping process has no noticeable effect on the nanosheet structure. The transmission electron microscope (TEM) image reveals that the nanosheets are formed by multiple closely-packed single crystals (Fig.1d). The high resolution TEM (HRTEM) image shows that these nanosheets are mainly bounded with Co_3O_4 {111} facets (Fig. 1e), further confirming the well-maintained bulk Co_3O_4 crystals after VPH doping.

Fig, 2a shows the X-ray photoelectron spectroscopy (XPS) data of CNS and S-CNS samples. The measured surface contents of S-CNS by XPS are Co 15.25%, O 11.55%, S 47.22%, C 24.81% and Sn 1.17% (from FTO). The confirmed 47% surface doped S content without affecting the bulk Co_3O_4 crystal structure is unprecedented as the S contents of S-doped metal oxides published to date are less than 10% due to the destruction of high contents of doped S to the original metal oxide crystal structures.[13] The effectiveness and superiority of the VPH doping approach can be attributed to the unique H_2S-rich vapour reaction environment that enables a selective surface doping at mild conditions (90°C).

The high-resolution Co $2p_{3/2}$ spectra (Fig. 2b) can be fitted to three main peaks and several weak shake-up satellite peaks (referred to Co (II) in high spin state). The split spin-orbit of 2p (ΔE) are 15 eV for both samples, consistent with the reported values for Co_3O_4 crystals. The Co $2p_{3/2}$ peak (centred at 779.9 eV) is shifted to 779.3 eV, close to that of Co_3S_4 (779.0 eV).[14] For the O 1s spectra (Fig. 2c), the peak centred at 529.6 observed from CNS can be assigned to the lattice oxygen (O_{lat}, Co-O) and the rest of the peaks are attributed to absorbed non-stoichiometric oxygen. Notably, the O_{lat} peak of S-CNS vanishes while others shift towards higher binding energies. Importantly, the surface O replacement by S can be confirmed from the observed main S $2p_{3/2}$ peak centred at 162.4eV (assigned to Co-S) and the minor peak centred at 163.5eV (related to S_n^{2-} species) from S-CNS (Fig. 2d).

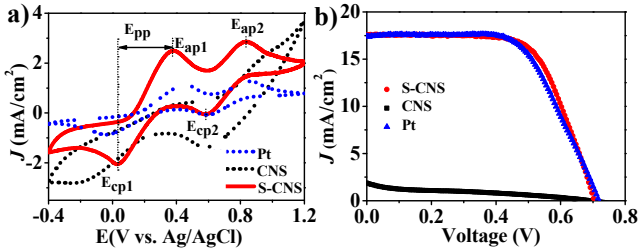

Fig. 3 (a) CVs of CNS, S-CNS and Pt electrodes in I^-/I_3^- electrolyte. (b) *J-V* curves of DSSCs with CNS, S-CNS and Pt counter electrodes.

The electrocatalytic activity of S-CNS electrode was evaluated for the most commonly employed I^-/I_3^- electrolyte system in dye-sensitised solar cells (DSSCs). The cyclic voltammogram (CV) of CNS electrode in I^-/I_3^- solution shows ill-defined I^-/I_3^- redox responses, indicating a poor reversibility and electrocatalytic activity (Fig. 3a). In strong contrast, the CV of S-CNS electrode obtained under the same conditions reveals two pairs of well-defined redox peaks, representing the distinctive characteristic of I^-/I_3^- redox processes, confirming the superior electrocatalytic activity of S-CNS (Fig. 3a). Comparing to Pt (Fig. 3a) and metal sulphide electrodes (e.g., NiS, MoS, Co_3S_4 and Ni_3S_4),[15, 16] S-CNS electrode exhibits a noticeable anodically shifted cathodic peak potential and significantly reduced redox peak separation (E_{pp}=E_{ap1}-E_{cp1}) corresponding to I^-/I_3^- redox processes, further confirming the superiority of S-CNS. The excellent electrochemical stability of S-CNS electrode is demonstrated by the almost identical CV responses obtained from 100 consecutive cycles (Fig. S3).

The electrocatalytic activity of S-CNS as a counter electrode in DSSC was also evaluated (Fig.3b). The key performance parameters are summarised in Table S1. The DSSC assembled with the S-CNS counter electrode shows a conversion efficiency of 7.79%, almost identical to that of the DSSC assembled with a benchmark Pt counter electrode

(7.81%), and higher than those assembled using S-doped nickel oxide[17] and metal sulphides counter electrodes.[15, 18]

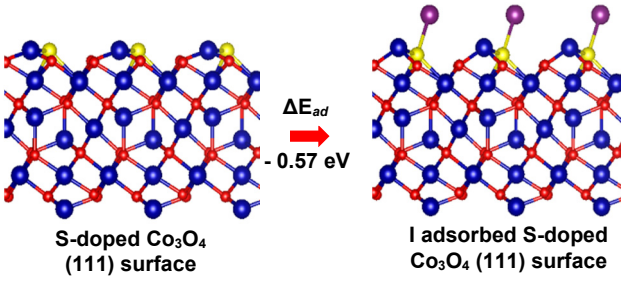

Fig. 4 Schematic illustration of the atomic arrangements of the clean and I adsorbed S-doped Co_3O_4 (111) surface. Atoms in blue, red, yellow and purple colours represent Co, O, S and I, respectively.

The results shown in Fig. 3 suggest that only S-doped (rather than the pristine) {111} faceted Co_3O_4 is electrocatalytically active. The possible origin of electrocatalytic activity for S-doped {111} faceted Co_3O_4 towards I_3^- reduction is therefore investigated using Density functional theory (DFT). Previous studies have shown that a high performance electrocatalyst for I_3^- reduction reaction should possess optimal I adsorption energies (ΔE_{ad}) between -0.33 and -1.20 eV.[2a] The XPS results (Fig. 2) suggest that the surface S doping is achieved by forming Co-S bonds via surface O substitution. The optimised structure of the S-doped Co_3O_4 (111) surface is shown in Fig. 4. The calculated ΔE_{ad} of I on such optimised surface is -0.57 eV, close to ΔE_{ad} values obtained from Pt (-0.52 eV) and CoS (-0.59 eV) surfaces.[2a] This indicates that the surface Co-S bonds resulted from VPH doping should be the main form of surface active sites.

In summary, the effectiveness of VPH approach has been validated for *in situ* selective doping of exceptionally high S contents onto the surface of Co_3O_4 crystal without destruction to the bulk structures. The obtained electrocatalyst exhibits superior electrocatalytic activity for I_3^- reduction, almost identical to that of the benchmark commercial Pt catalyst. The VPH surface doping approach demonstrated in this work is simple, effective and directly applicable to a wide spectrum of metal oxides-based electrocatalysts for other applications such as hydrogen and oxygen evolution reactions.

This work is supported by Australian Research Council (Future Fellow Project) and Natural Science Foundation of China (51372248).

Notes and references

[a] *Centre for Clean Environment and Energy, Griffith University, Gold Coast Campus, QLD, 4222, Australia.*
E-mail: h.zhao@griffith.edu.au; p.liu@griffith.edu.au.
[b] *Key Laboratory of Materials Physics, Centre for Environmental and Energy Nanomaterials, Institute of Solid State Physics, Chinese Academy of Sciences, P.O. Box 1129, Hefei 230031, P.R. China*

† Electronic Supplementary Information (ESI) available: experimental section and characterisations. See DOI: 10.1039/b000000x/

1 (a) B. Winther-Jensen and D. R. MacFarlane, *Energy Environ. Sci.*, 2011, **4**, 2790; (b) M. S. Faber and S. Jin, *Energy Environ. Sci.*, 2014, **7**, 3519.

2 (a) Y. Hou, D. Wang, X. H. Yang, W. Q. Fang, B. Zhang, H. F. Wang, G. Z. Lu, P. Hu, H. J. Zhao and H. G. Yang, *Nat. Commun.*, 2013, **4**, 1583; (b) B. Zhang, D. Wang, Y. Hou, S. Yang, X. H. Yang, J. H. Zhong, J. Liu, H. F. Wang, P. Hu, H. J. Zhao and H. G. Yang, *Sci. Rep.*, 2013, **3**, 1836; (c) A. P. O'Mullane, *Nanoscale*, 2014, **6**, 4012.

3 (a) K. Gong, F. Du, Z. Xia, M. Durstock and L. Dai, *Science*, 2009, **323**, 760; (b) B. Zhang, N. N. Zhang, J. F. Chen, Y. Hou, S. Yang, J. W. Guo, X. H. Yang, J. H. Zhong, H. F. Wang, P. Hu, H. J. Zhao and H. G. Yang, *Sci. Rep.*, 2013, **3**; (c) B. Xia, Y. Yan, X. Wang and X. W. Lou, *Mater. Horiz.*, 2014, **1**, 379; (d) Y. Li, H. Zhang, Y. Wang, P. Liu, H. Yang, X. Yao, D. Wang, Z. Tang and H. Zhao, *Energy Environ. Sci.*, 2014, **7**, 3720.

4 (a) M. K. Datta, K. Kadakia, O. I. Velikokhatnyi, P. H. Jampani, S. J. Chung, J. A. Poston, A. Manivannan and P. N. Kumta, *J. Mater. Chem. A*, 2013, **1**, 4026; (b) S. Y. Yang, Y. S. Choo, S. Kim, S. K. Lim, J. Lee and H. Park, *Appl. Catal., B*, 2012, **111–112**, 317.

5 F. Wang, Y. Han, C. S. Lim, Y. Lu, J. Wang, J. Xu, H. Chen, C. Zhang, M. Hong and X. Liu, *Nature*, 2010, **463**, 1061.

6 (a) A. Gasparotto, D. Barreca, D. Bekermann, A. Devi, R. A. Fischer, P. Fornasiero, V. Gombac, O. I. Lebedev, C. Maccato, T. Montini, G. Van Tendeloo and E. Tondello, *J. Am. Chem. Soc.*, 2011, **133**, 19362; (b) Z. Mei, Z. Shen, W. Wang and Y. Zhang, *Environ. Sci. Technol.*, 2007, **42**, 590.

7 C.-H. Cui and S.-H. Yu, *Acc. Chem. Res.*, 2013, **46**, 1427.

8 (a) H. Zhao, Y. Shen, S. Zhang and H. Zhang, *Langmuir*, 2009, **25**, 11032; (b) P. Liu, H. Zhang, H. Liu, Y. Wang, X. Yao, G. Zhu, S. Zhang and H. Zhao, *J. Am. Chem. Soc.*, 2011, **133**, 19032; (c) H. Zhang, Y. Li, P. Liu, Y. Li, D. Yang, H. Yang and H. Zhao, *Chem. -Eur. J.*, 2012, **18**, 5165.

9 (a) X. Wang, W. Tian, T. Zhai, C. Zhi, Y. Bando and D. Golberg, *J. Mater. Chem.*, 2012, **22**, 23310; (b) H. Sun, H. M. Ang, M. O. Tade and S. Wang, *J. Mater. Chem. A*, 2013, **1**, 14427.

10 H. Yu, Y. Li, X. Li, L. Fan and S. Yang, *Chem. -Eur. J.*, 2014, **20**, 3457.

11 S. Y. Bae, H. W. Seo and J. Park, *J. Phys. Chem. B*, 2004, **108**, 5206.

12 V. G. Hadjiev, M. N. Iliev and I. V. Vergilov, *J. Phys. C.: Solid State Phys.*, 1988, **21**, L199.

13 (a) G. K. Pradhan, N. Sahu and K. M. Parida, *RSC Adv.*, 2013, **3**, 7912; (b) M. H. Z. Maha, M. M. Bagheri-Mohagheghi, H. Azimi-Juybari and M. Shokooh-Saremi, *Phys. Scr.*, 2012, **86**, 055701.

14 Q. Wang, L. Jiao, H. Du, Y. Si, Y. Wang and H. Yuan, *J. Mater. Chem.*, 2012, **22**, 21387.

15 J. Yang, C. Bao, K. Zhu, T. Yu, F. Li, J. Liu, Z. Li and Z. Zou, *Chem. Commun.*, 2014, **50**, 4824.

16 (a) Y. Li, H. Wang, H. Zhang, P. Liu, Y. Wang, W. Fang, H. Yang, Y. Li and H. Zhao, *Chem. Commun.*, 2014, **50**, 5569; (b) M. Al-Mamun, H. Zhang, P. Liu, Y. Wang, J. Cao and H. Zhao, *RSC Adv.*, 2014, **4**, 21277.

17 G. H. Guai, M. Y. Leiw, C. M. Ng and C. M. Li, *Adv. Energy Mater.*, 2012, **2**, 334.

18 (a) H. Sun, D. Qin, S. Huang, X. Guo, D. Li, Y. Luo and Q. Meng, *Energy Environ. Sci.*, 2011, **4**, 2630; (b) M. Wang, A. M. Anghel, B. Marsan, N.-L. Cevey Ha, N. Pootrakulchote, S. M. Zakeeruddin and M. Grätzel, *J. Am. Chem. Soc.*, 2009, **131**, 15976.